JOURNAL OF COMPUTATIONAL PHYSICS 110, 327–340 (1994)

The Δ-ϵ Method for the Boltzmann Equation

ZHIQIANG TAN AND PHILIP L. VARGHESE

Center for Aeromechanics Research, Department of Aerospace Engineering and Engineering Mechanics, The University of Texas at Austin, Austin, Texas 78712

Received February 1, 1993

A new numerical method is proposed to solve the Boltzmann equation. A frame is set up by using a discrete velocity approximation in the infinite velocity space, but by considering only those distribution function points which are not too small. The distribution function points may occur anywhere in the infinite discrete velocity space and are not constrained to a pre-specified region. A fourth-order finite difference is used for the convection terms. A Monte Carlo-like method is applied to the discrete velocity model of the collision integral. The effort of the method is proportional to the number of discrete points. Numerical examples are given for the full Boltzmann equation and results for some benchmark problems are compared with analytical or prior solutions.

1. INTRODUCTION

The Boltzmann equation is the basis of rarefied gas dynamics. Its applications can be found in many areas ranging from flight simulations of high altitude vehicles to separation of isotopes. Because of its nonlinearity and multi-dimensionality, analytical solutions of the Boltzmann equation have been found only for very few limiting cases. Numerical methods must be invoked for most practical problems.

Many deterministic computational techniques, used successfully in areas such as fluid dynamics and neutron transport, have been attempted on the Boltzmann equation. Examples include the finite difference method (FDM) [1] and the finite element method (FEM) [2]. Unfortunately, most methods work well only for the linearized Boltzmann equation or model equations. Only probabilistic Monte Carlo techniques have been used successfully for the full nonlinear Boltzmann equation. Examples are the direct simulation Monte Carlo (DSMC) method described by Bird [3] and the modified Nanbu's Monte Carlo method [4, 5].

Monte Carlo simulation methods have been applied to very complex problems, e.g., multidimensional chemically reacting flow of polyatomic gases, but several weaknesses have restricted their efficiency. Monte Carlo techniques suffer from statistical fluctuations and their convergence rate is quite low (of order $N^{-1/2}$, where N is the number of simulating particles). The convergence rate of the simulation methods is very slow for flows with large spatial variations in Knudsen number because of their inefficiency for continuum flows ($\mathrm{Kn} \ll 1$). Because of the particle feature of the simulation techniques it is difficult to match them to a Navier–Stokes solver. This inhibits the use of the Navier–Stokes equations in flow domains where Kn is small and the Boltzmann solvers are inefficient.

Discrete velocity approximations are used in another class of numerical methods, e.g., the Hicks–Yen–Nordsiek (HYN) method [6, 7]. In the HYN method, the collision integral is calculated by a Monte Carlo method. The convection term is approximated by a first-order upwind finite difference. Although the method is more deterministic than particle simulation techniques it requires some correction scheme to enforce conservation of mass, momentum, and energy. These quantities are not accurately conserved because the collision integral is only evaluated approximately. One advantage of the HYN method is that mixed continuum and rarefied flow problems can be solved more easily [8]. Another advantage is that an implicit scheme can be applied to steady state problems, permitting larger time steps and faster convergence. Similar advantages and disadvantages also apply to other methods of this class (e.g., [9, 10]).

A major problem associated with the discrete velocity approximation in the HYN class methods is that the infinite velocity space is approximated by a finite region, and all points in that region are considered. For low Mach number flows this is no problem because the distribution function is significant only in a small region of velocity space. A large box is needed to confine the region where the distribution function is significant at large Mach numbers because the distribution function is bimodal. Freestream molecules tend to be distributed about the large freestream velocity, whereas molecules that have struck the surface tend to be distributed about zero velocity. The problem cannot be resolved by using a coarser mesh in velocity space. The mesh size must be similar for both low and high Mach

581/110/2-9

0021-9991/94 $6.00

number problems for comparable accuracy. Hence many more grid points are required for high Mach number problems, which greatly increases the computing effort.

We are developing a new numerical technique, the Δ-ε method, for the Boltzmann equation. In Sections 2 and 3, the formulation and the so-called Δ-ε frame and some basic operations are described. The treatment of the convective terms is given in Section 4. The numerical scheme for the collision process and its implementation in the Δ-ε frame are outlined in Section 5. The error analyses for simple cases are presented in Section 6. Finally, some example problems are shown in Section 7.

2. FORMULATION

Assuming there is no external body force, the dimensionless Boltzmann equation for rarefied flow of a single component monatomic gas in 2D physical space is

$$\frac{Df}{Dt} \equiv \frac{\partial f}{\partial t} + \nabla_{\mathbf{r}} \cdot (\mathbf{v} f) = I \tag{1a}$$

with

$$I \equiv \frac{1}{\mathrm{Kn}} \int_{S^2} \frac{d\Omega}{4\pi} \int_{\mathbb{R}^3} [f(\mathbf{r}, \mathbf{v}', t)\, f(\mathbf{r}, \mathbf{w}', t) - f(\mathbf{r}, \mathbf{v}, t)\, f(\mathbf{r}, \mathbf{w}, t)]\, g\sigma(g, \theta)\, d\mathbf{w}, \tag{1b}$$

where $f = f(\mathbf{r}, \mathbf{v}, t)$ is the velocity distribution function normalized to the number density, $\mathbf{r} = (r_1, r_2, r_3)$ is the position vector in physical space, $\mathbf{v} = (v_1, v_2, v_3)$ is the velocity vector, and t is the time. $S^2 = \{\mathbf{x} \in \mathbb{R}^3 \mid \|\mathbf{x}\| = 1\}$ denotes the surface of the unit sphere, where $\|\mathbf{x}\| \equiv (\mathbf{x} \cdot \mathbf{x})^{1/2}$. The relative speed g is given by $\|\mathbf{v} - \mathbf{w}\|$. The quantities θ, $\mathbf{v}'$, $\mathbf{w}'$, and σ are binary collision parameters; θ is the deflection angle, $\mathbf{v}'$ and $\mathbf{w}'$ are the post-collisional velocities of $\mathbf{v}$ and $\mathbf{w}$, respectively, and $\sigma = \sigma(g, \theta)$ is the differential cross section for binary collisions. The Knudsen number Kn is defined by $\mathrm{Kn} = \lambda / L$ with $\lambda = 1/(\sqrt{2}\, n_0 \sigma_0)$. Here λ is the mean free path, L is the characteristic length, and σ_0 is a reference cross section. The cross section can be estimated by Chapman–Enskog theory [11] for hard sphere molecules, i.e., $\sigma_0 = 5(\pi m k T_0)^{1/2} / 16 \mu_0$, where m is the mass of the molecule, k is Boltzmann's constant, T_0 is the reference temperature, and μ_0 is the viscosity of the gas at T_0. For simplicity, the variable hard sphere (VHS) model of Bird [12] is used for the differential cross section, i.e., $g\sigma(g, \theta) = C_\kappa g^{1 - 4/\kappa}$, where κ is the exponent in the intermolecular potential and $C_\kappa = 3\sqrt{2}\,(2-\alpha)^{-\alpha} / \Gamma(4-\alpha)$ with $\alpha \equiv 2/\kappa$. The characteristic parameters for $\mathbf{r}$, $\mathbf{v}$, t, and f were chosen to be

$$r_0 = L, \qquad v_0 = \sqrt{2RT_0}, \qquad t_0 = \frac{x_0}{v_0}, \qquad f_0 = \frac{n_0}{v_0^3},$$

where R is the gas constant and n_0 the characteristic number density.

Equation (1) can also be written in weak form as (see, e.g., Cercignani [13])

$$\int_{\mathbb{R}^3} \frac{Df}{Dt} \varphi(\mathbf{v})\, d\mathbf{v} = \frac{1}{2\,\mathrm{Kn}} \int_{S^2} \frac{d\Omega}{4\pi} \int_{\mathbb{R}^3} \int_{\mathbb{R}^3} [\varphi(\mathbf{v}') + \varphi(\mathbf{w}') - \varphi(\mathbf{v}) - \varphi(\mathbf{w})]\, f(\mathbf{v})\, f(\mathbf{w})\, g\sigma(g, \theta)\, d\mathbf{v}\, d\mathbf{w}, \tag{2}$$

where $\varphi(\mathbf{v})$ is a test function. Specifically, if $\varphi(\mathbf{v})$ is taken as the Dirac delta function $\delta^3(\mathbf{v} - \mathbf{u})$, then Eq. (2) reduces to

$$\frac{Df(\mathbf{r}, \mathbf{u}, t)}{Dt} = \frac{1}{2\,\mathrm{Kn}} \int_{S^2} \frac{d\Omega}{4\pi} \int_{\mathbb{R}^3} \int_{\mathbb{R}^3} [\Delta_{\mathbf{v}} + \Delta_{\mathbf{w}}] \times f(\mathbf{v})\, f(\mathbf{w})\, g\sigma(g, \theta)\, d\mathbf{v}\, d\mathbf{w}, \tag{3}$$

where $\Delta_{\mathbf{v}} = \delta^3(\mathbf{v}' - \mathbf{u}) - \delta^3(\mathbf{v} - \mathbf{u})$ and $\Delta_{\mathbf{w}} = \delta^3(\mathbf{w}' - \mathbf{u}) - \delta^3(\mathbf{w} - \mathbf{u})$. Equation (3) is equivalent to the original Boltzmann equation and is suitable for deriving various numerical schemes such as the one in this paper and most particle simulation schemes.

3. THE Δ-ε FRAME

In this section we shall omit the dependence of f on $\mathbf{r}$ and t for compactness because only changes in the velocity space are considered.

In common with the discrete velocity method [9, 10, 14], we partition the infinite space $\mathbb{R}^3$ into an infinite number of cubic elements $e_{\mathbf{i}}$ ($\mathbf{i} \in \mathbb{Z}^3$) of equal size, with side Δv. Depending on the position of the origin in a cell, the discrete model may be even or odd, where

$$e_{\mathbf{i}} = \left\{ \mathbf{v} \,\middle|\, |v_k - i_k\, \Delta v| < \frac{\Delta v}{2},\ k = 1, 2, 3 \right\} \text{—even;}$$

$$e_{\mathbf{i}} = \left\{ \mathbf{v} \,\middle|\, \left| v_k - \left(i_k + \frac{1}{2} \right) \Delta v \right| < \frac{\Delta v}{2},\ k = 1, 2, 3 \right\} \text{—odd.}$$

Without loss of generality, only the even model will be considered in this and the following two sections.

In each element $e_{\mathbf{i}}$, the simplest particle-like approximation of the distribution function is considered,

$$f(\mathbf{v}) = \Delta v^3\, \delta^3(\mathbf{v} - \mathbf{v}_{\mathbf{i}})\, f_{\mathbf{i}}, \qquad \mathbf{v} \in e_{\mathbf{i}}, \tag{4}$$

where δ is the Dirac delta function, $f_{\mathbf{i}} \equiv f(\mathbf{v}_{\mathbf{i}})$ and $\mathbf{v}_{\mathbf{i}} \equiv \mathbf{i}\, \Delta v$.

Of course only a finite number of elements can be considered in numerical calculation. In the HYN class methods a regular finite region (say a square box) is used. This region

must be big enough so that all distribution function points lying outside the finite region can be ignored. As indicated in the Introduction, this may require excessive computer time and memory for large Mach number problems.

Note that in Bird's method or Nanbu's method there is no artificial boundary in velocity space. In fact the simulating particles are allowed to have any velocity. They are more efficient in discretization than the HYN class methods because the regions in velocity space, where only a few particles exist will not be sampled. This is in contrast to the HYN class methods where all distribution function points inside the box are considered.

The above arguments suggested that we develop a new method which considers only the significant points and eliminates the finite velocity space approximation, while maintaining the features of the discrete velocity approximation. For a distribution $f \equiv \{f_{\mathbf{i}}, \mathbf{i} \in \mathbb{Z}^3\}$, we retain only those elements in which the distribution function is greater than a prescribed threshold, f_ε (>0) (Fig. 1). Therefore, the *important distribution* of f can be defined as $F \equiv \{f_{\mathbf{i}} > f_\varepsilon, \mathbf{i} \in \mathbb{Z}^3\}$. We denote the transformation from f to F by $\bar{\mathrm{I}}$, i.e., $F = \bar{\mathrm{I}} f$. Since the density cannot be infinite, the number of elements of F, denoted by N, is finite. Obviously, N and the domain of F depend on the distribution f, Δv, and f_ε. These quantities can change in physical space and time. F can be remapped as a 1D array $\{(f_i, \mathbf{v}_i), i = 1, ..., N\}$. In a computer program, F is recorded by two arrays L(3, NV) and F(NV), as well as the number N, where L is the position array which stores the three components of the position in discrete velocity space of each important distribution function value at a point in physical space, $\mathrm{NV} \geqslant N$ is a pregiven number, and F is the value of the important distribution at each point. Since NV is fixed and N varies with space and time, there will be some memory waste.

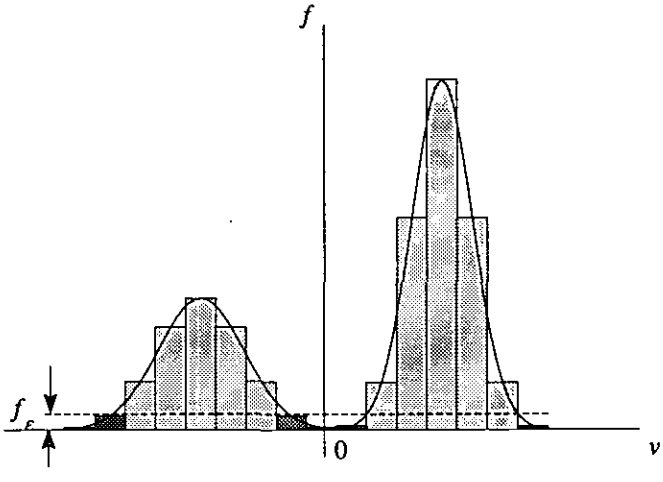

FIG. 1. Approximation of the distribution function f in the discrete velocity space. The bars denote the discrete distribution functions. The darker bars are the *unimportant distribution functions* that lie below f_ε and should be truncated. The scale of f_ε has been exaggerated for clarity.

However, by using a sophisticated data structure, significant reduction in memory size is possible.

In this framework the integration of the Boltzmann equation describes the evolution of the important distribution function points in physical and velocity space. Several basic operations on important distributions are used frequently. These include sorting, merging, truncating the unimportant distribution function points, multiplying an important vector by a constant, and computing the moments of an important distribution function vector. We briefly describe the sorting and merging operations below:

(1) *Sorting.* As we shall see, the integration of the Boltzmann equation can be decomposed into summations or subtractions of important distributions. Since it is more convenient to work on ordered distributions, the sorting procedure is necessary. An important distribution $\{(f_i, \mathbf{v}_i), i = 1, ..., N\}$ is said to be ordered if $V_j < V_k$ for all $j < k$, where

$$V_j = (v_{j,3} + S)(2S+1)^2 + (v_{j,2} + S)(2S+1) + v_{j,1} + S + 1$$

and $S > \max(|v_{j,m}|, 1 \leqslant j \leqslant N, 1 \leqslant m \leqslant 3)$ is a sufficiently large constant. We use the above definition because inverse transformations, i.e., obtaining $\mathbf{v}_j$ for given V_j, are also easy to calculate. The sorting procedure has been thoroughly studied in computer science and algorithms can be found in many textbooks (e.g., [15]).

(2) *Merging.* The merging procedure $\bar{\mathrm{M}}$, maps two (or more) ordered important distributions $F = \{(f_i, \mathbf{v}_i), i = 1, ..., N_f\}$ and $G = \{(g_i, \mathbf{v}_i), i = 1, ..., N_g\}$ into an ordered $H = \{(h_i, \mathbf{v}_i), i = 1, ..., N_h\}$ such that

$$h_i = \begin{cases} f_i + g_i & \text{if } (f_i, \mathbf{v}_i) \in F \text{ and } (g_i, \mathbf{v}_i) \in G \\ f_i & \text{if } (f_i, \mathbf{v}_i) \in F \text{ and } (g_i, \mathbf{v}_i) \notin G \\ g_i & \text{if } (f_i, \mathbf{v}_i) \notin F \text{ and } (g_i, \mathbf{v}_i) \in G \end{cases}$$

We denote this procedure by $H = \bar{\mathrm{M}}(F, G)$. The algorithm for this procedure is straightforward and will not be elaborated here.

There are two main features of the present technique for computing the Boltzmann equation: (i) the velocity space is discretized into elements with side Δv, and (ii) only those distribution function values which are greater than f_ε are retained. Hence, we call our frame the Δv-f_ε frame or, briefly, the Δ-ε frame. Many computational schemes for the left or right side of the Boltzmann equation can be implemented in this frame. Although the frame is useful because it eliminates calculations of the unimportant points, it is essential that efficient schemes that are implementable in the frame be used.

The principle of the Δ-ε frame can be extended in a straightforward fashion to higher microscopic dimensions

to include velocity, species, and internal energy variables, in which only those points which are important in the discrete velocity-species-internal energy space are retained. The idea can be also applied to many other transport equations such as the Fokker–Planck equation and the Vlasov equation.

4. APPROXIMATION OF THE COLLISIONLESS PROCESS AND IMPLEMENTATION IN THE Δ-ε FRAME

We can split the time integration in Δt into a collisionless process and a homogeneous collision process. This makes the program more modular. In this section, we study the collisionless process only. We shall use a structured grid and finite difference for the spatial derivatives. However, the Δ-ε frame is also suitable for finite element or finite volume methods.

Consider the 1D equation

$$\frac{\partial f}{\partial t}+\mathrm{v}\frac{\partial f}{\partial x}=0 \tag{5}$$

in $(n\,\Delta t, (n+1)\,\Delta t]$, where $v=v_1$. We prefer explicit schemes because they are easier to implement in the Δ-ε frame. However, the implicit first-order upwind scheme can also be implemented. In our work, the following centered fourth-order scheme is used,

$$f_i^+=\alpha_{-2}f_{i-2}+\alpha_{-1}f_{i-1}+\alpha_0 f_i+\alpha_1 f_{i+1}+\alpha_2 f_{i+2}, \tag{6}$$

where $f_i^+=f(i\,\Delta x, \mathbf{v}, (n+1)\,\Delta t)$, $f_{i+k}=f((i+k)\,\Delta x, \mathbf{v}, n\,\Delta t)$ $(k=-2, ..., +2)$, $\alpha_0=(1-c^2)(4-c^2)/4$, $\alpha_{\pm 1}=(-1\pm c)(-4+c^2)/6$, and $\alpha_{\pm 2}=(1-c^2)(-2\pm c)/24$; $c=v\,\Delta x/\Delta t$ is the CFL number. The scheme is stable if $|c|<1$.

In the Δ-ε frame, the above equation becomes

$$\begin{aligned}\bar{\mathrm{I}}f_i^+&=\bar{\mathrm{I}}(\alpha_{-2}f_{i-2}+\alpha_{-1}f_{i-1}+\alpha_0 f_i+\alpha_1 f_{i+1}+\alpha_2 f_{i+2})\\&\approx\bar{\mathrm{M}}[\alpha_{-2}\bar{\mathrm{I}}f_{i-2}, \alpha_{-1}\bar{\mathrm{I}}f_{i-1}, \alpha_0\bar{\mathrm{I}}f_i, \alpha_1\bar{\mathrm{I}}f_{i+1}, \alpha_2\bar{\mathrm{I}}f_{i+2}]\end{aligned} \tag{7}$$

which can be calculated with the merging procedure. The scheme can be extended easily to multiple dimensions in physical space with curvilinear coordinates.

5. APPROXIMATION OF THE COLLISION INTEGRAL

For simplicity, VHS molecules are assumed. From (3) and (4), the collision integral at $\mathbf{v}$ in the discrete velocity space is

$$\begin{aligned}I&=\frac{C_\kappa\,\Delta v^6}{2\,\mathrm{Kn}}\sum_{i=1}^{N}\sum_{j=1}^{N}f_i f_j\int_{S^2}[\Delta_i+\Delta_j]\,g_{ij}^{1-4/\kappa}\frac{d\Omega}{4\pi}\\&\equiv A-B,\end{aligned} \tag{8}$$

where $\Delta_i=\delta^3(\mathbf{v}_i'-\mathbf{v})-\delta^3(\mathbf{v}_i-\mathbf{v})$, $\Delta_j=\delta^3(\mathbf{v}_j'-\mathbf{v})-\delta^3(\mathbf{v}_i-\mathbf{v})$, and A and B represent the replenishing and depleting terms, respectively. The homogeneous collision process is governed by

$$f^+=f+\Delta t\,I, \tag{9}$$

where f and f^+ are defined at t_0 and $t_0+\Delta t$, respectively. To obtain the new important distribution $\bar{\mathrm{I}}f^+$, we need to express f^+ in the form of Eq. (4).

Generally the post-collisional velocities do not lie on the grid for an arbitrary direction $\mathbf{s}\in S^2$. Therefore, the kinetic energy is not always conserved. However, energy conservation can be enforced if we approximate the angular integral in Eq. (8) by numerical quadrature taking the numerical integration points to be *exactly* on a restricted number of appropriate grid points. Thus

$$\int_{S^2}[\Delta_i+\Delta_j]\frac{d\Omega}{4\pi}=\sum_{l=1}^{M_{ij}}w_l[\Delta_i+\Delta_j], \tag{10}$$

where M_{ij} is the total number of such integration points and depends on $\mathbf{v}_i$ and $\mathbf{v}_j$, and w_l are weights (Fig. 2). The directions $\mathbf{s}_l$, or equivalently, the post-collision velocities, are shown in Fig. 2. The weights could be constructed according to i and j for maximum accuracy, but this is tedious and rather expensive. We assume that the $\mathbf{s}_l$ are evenly distributed on S^2. Therefore, w_l can be approximated by

$$w_l=1/M_{ij} \tag{11}$$

and the collision integral reduces to

$$I=\sum_{i=1}^{N}\sum_{j=1}^{N}\frac{C_\kappa\,\Delta v^6}{2\,\mathrm{Kn}\,M_{ij}}\,g_{ij}^{1-4/\kappa}f_i f_j\sum_{l=1}^{M_{ij}}[\Delta_i+\Delta_j]. \tag{12}$$

This is equivalent to the discrete velocity formulation used by Goldstein *et al.* [14] and Inamuro and Sturtevant [10] who obtained it from a very different point of view.

A table of the discrete points are pre-calculated and stored to reduce computer time. The procedures for generating the table and retrieving the post-collisional velocities from it are given in Appendix A.

The evaluation of the distribution of I would require an effort of $O(N^2)$. To reduce the effort to $O(N)$, we approximate the triple summation by a single summation using a Monte Carlo method.

We rewrite Eq. (12) as

$$I=\frac{C_\kappa\rho^2}{2\,\mathrm{Kn}\,M_{ij}}\sum_{i=1}^{N}\sum_{j=1}^{N}p_i p_j\sum_{l=1}^{M_{ij}}[\Delta_i+\Delta_j]\,g_{ij}^{1-4/\kappa}, \tag{13}$$

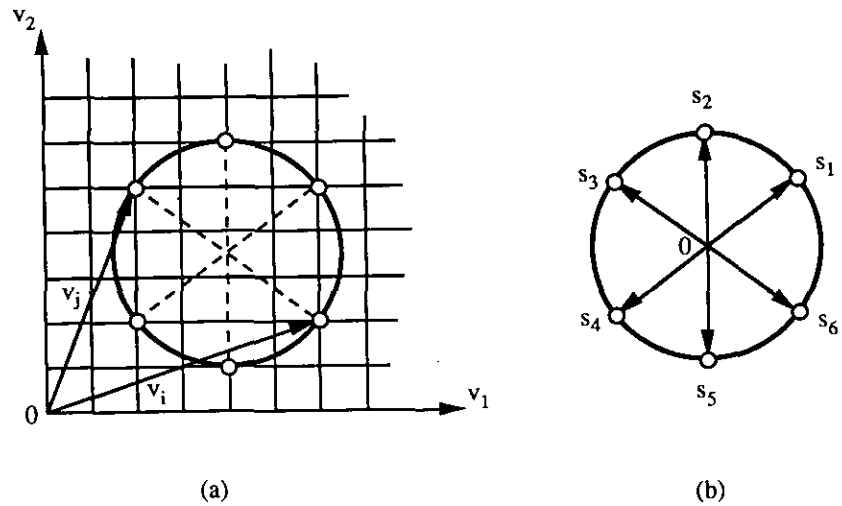

FIG. 2. (a) Selection of the post-collisional velocities and (b) corresponding integral points for the angular integral.

where $p_i = f_i \Delta v^3/\rho$ is the probability that a particle is found at $\mathbf{v}_i$ and ρ is the local density. For a given integer $M > 0$, we first choose a set of i_r and j_r $(r = 1, ..., M)$ according to the probability p_i. We use an "alias method" [16] to choose i_r and j_r. This method is very efficient and requires only $O(M)$ operations. Then for each pair of (i_r, j_r) a direction $\mathbf{s}_r$ is chosen randomly from the table of all the $M_{i_r j_r}$ possible discrete directions. Therefore, Eq. (13) is approximated by

$$I(\mathbf{v}) \approx \frac{C_\kappa \rho^2}{2\,\mathrm{Kn}\, M} \sum_{r=1}^{M} [\Delta_{i_r} + \Delta_{j_r}]\, g_{i_r j_r}^{1-4/\kappa}. \tag{14}$$

This can always be expressed in the form $\sum c_k\, \delta^3(\mathbf{v}_k - \mathbf{v})$, $k = 1, ..., N^+$, for some N^+ by collecting the coefficients of the delta functions in (14). We use the following procedure:

a. For $r = 1, ..., M$,

(i) Select i and j from p_i;

(ii) Select the post-collision velocities $\mathbf{v}_i'$ and $\mathbf{v}_j'$ according to the table;

(iii) Calculate $a \equiv (C_\kappa \rho^2/2\,\mathrm{Kn}\, M)\, g_{i_r j_r}^{1-4/\kappa}$:

$$\mathbf{a}_r \leftarrow \mathbf{v}_i',\ f_{a,r} \leftarrow a; \qquad \mathbf{b}_r \leftarrow \mathbf{v}_j',\ f_{b,r} \leftarrow a;$$
$$\mathbf{c}_r \leftarrow \mathbf{v}_i,\ f_{c,r} \leftarrow a; \qquad \mathbf{d}_r \leftarrow \mathbf{v}_j,\ f_{d,r} \leftarrow a.$$

b. Sort $F_a \equiv \{(f_{a,r}, \mathbf{a}_r),\ r = 1, ..., M\}$ and $F_b \equiv \{(f_{b,r}, \mathbf{b}_r),\ r = 1, ..., M\}$ (no sorting is needed for $F_c \equiv \{(f_{c,r}, \mathbf{c}_r),\ r = 1, ..., M\}$ and $F_d \equiv \{(f_{d,r}, \mathbf{d}_r), r = 1, ..., M\}$ because they are already ordered in the collisionless step).

c. Apply the merging procedure to calculate $\bar{I}I = \bar{M}[F_a, -F_b, F_c, -F_d]$. When the important collision integral distribution is calculated, the important distribution at the new time step is simply $\bar{I}f = \bar{M}[\bar{I}f, \bar{I}I]$.

Remarks. a. In approximating the angular integral, we have introduced two approximations: (i) the integral points must be on the grid, and (ii) the integral points are uniformly distributed on the unit sphere. The first approximation does not introduce convergence problems if we can prove that when $\Delta v \to 0$, the number of such integral points is infinite and dense on the sphere. The second approximation is also compatible if one can prove that the integral points tend to be uniformly distributed on the sphere as $\Delta v \to 0$. Unfortunately, the proofs involve some difficult problems in number theory and we are not aware of any solutions. However, the assumptions seem to be untuitively reasonable and numerical experiments are consistent with these assumptions.

b. In our work an explicit scheme for time integration has been used. An implicit scheme can also be applied, but the conservation laws are no longer satisfied exactly. In this case a correction scheme such as the method of Aristov and Cheremisin [17] might be applied. In our case, the time step Δt should be restricted by the requirement that no negative distribution function values should appear. For the exact discrete velocity formulation (Eq. (8)), this gives the following sufficient condition

$$f_i - \frac{\Delta v^6\, \Delta t}{2\,\mathrm{Kn}} \sum_{j=1}^{N} f_i f_j \sigma_{Tij}\, g_i \geqslant 0, \qquad \text{i.e.,} \quad \Delta t \leqslant \frac{2\,\mathrm{Kn}}{\Delta v^6 \sum_j f_j \sigma_{Tij}\, g_i}, \quad \forall 1 \leqslant i \leqslant N. \tag{15}$$

Here σ_{Tij} is the total cross section. However, even if the rather strict inequality (15) is enforced by using a small time step, the nonnegativity of the distribution function in the Δ-ε calculation is not guaranteed, because a Monte Carlo approximation has been used. Fortunately, there are very

few such points and the negative values are very small, so they can be tolerated or safely eliminated. In practice, a Δt larger than the limiting value from Eq. (15) can be used without introducing appreciable error.

c. Besides the discrete velocity model used here, many other models can also be used to approximate the collision integral in the Δ-ε frame. For example, the direction could change continuously on the unit sphere, and the piecewise-constant approximation rather than the piecewise-delta function approximation might be used for the distribution function.

d. Other sampling procedures are possible. For example, one may choose i and j based on the distribution $f_i f_j \sigma_{Tij} g_i$ rather than by $f_i f_j$ only. This might be done by the acceptance–rejection procedure and is similar to the DSMC methods.

e. The computing effort of the Δ-ε algorithm is easily seen to be proportional to M. In contrast to the direct simulation Monte Carlo methods, for which M represents the number of collisions and cannot be arbitrarily changed, the M in the Δ-ε method can be chosen quite freely according to the accuracy requirements and the local Knudsen number.

f. In our method, the pre-collision velocities are sampled in pairs, by virtue of the symmetric formulation of the collision integral. An unsymmetric formulation can also be used, but the momentum and energy conservations are not guaranteed. Our sampling method is closer to a particle simulation method than to the Monte-Carlo quadrature methods, e.g., the HYN method, that are more like a direct numerical integration.

6. ERROR ANALYSIS AND ESTIMATION OF Δv AND f_ε

When the computer roundoff error is negligible, the error of the present method in velocity space is induced by finite Δv (discretization) and f_ε (truncation of unimportant points). Estimation of the error in the general case is very difficult if not impossible. However, in the special case of a Maxwellian distribution, the error can be easily calculated. We believe that a study of this special case provides insight on the errors to be expected for more general problems.

Error Induced by Finite Δv

In this section we assume $f_\varepsilon = 0$, i.e., only the discretization error is considered. At equilibrium, $f_{\mathbf{i}'} f_{\mathbf{j}'} = f_{\mathbf{i}} f_{\mathbf{j}}$, where $\mathbf{i}'$ and $\mathbf{j}'$ are post-collision velocities conserving momentum and energy; i.e., $\mathbf{i}' + \mathbf{j}' = \mathbf{i} + \mathbf{j}$, $\mathbf{i}'^2 + \mathbf{j}'^2 = \mathbf{i}^2 + \mathbf{j}^2$, for all $\mathbf{i}, \mathbf{j} \in \mathbb{Z}^3$. The equilibrium distribution can be found in the same way as in the continuous velocity case [13]. The discrete velocity distribution that is invariant under collisions is

$$f_{\mathbf{i}}^* = \frac{\rho^*}{(\pi T^*)^{3/2}} \exp(-\mathbf{i}^2 \Delta v^2 / T^*), \tag{16}$$

where ρ^* and T^* are free parameters determined by the conditions

$$\rho = \Delta v^3 \sum_{\mathbf{i} \in \mathbb{Z}^3} f_{\mathbf{i}}^*, \qquad T = \Delta v^5 \sum_{\mathbf{i} \in \mathbb{Z}^3} \mathbf{i}^2 f_{\mathbf{i}}^*. \tag{17}$$

The true density and temperature given by Eq. (17) are not exactly the same as ρ^* and T^*, respectively. The relative differences $(\rho^* - \rho)/\rho$ and $(T^* - T)/T$ are only functions of the discretization parameter $s \equiv \Delta v / \sqrt{T}$ and are shown in Fig. 3. As expected, the differences vanish as s becomes zero, but it is remarkable that the differences are less than 0.1% when $s < 0.95$.

As a result of the above differences, there is also a difference between the discrete Maxwellian distribution $f_{\mathbf{i}}^*$ that uses ρ^* and T^* as parameters and the discrete Maxwellian distribution $f_{\mathbf{i}}$ that uses ρ and T as parameters. The difference in the distribution functions at $\mathbf{i} = \mathbf{0}$, $(f_0^* - f_0)/f_0$ is also a function of s alone and is also shown in Fig. 3.

It can be seen that when $s < 0.95$, all the errors are less than 0.1%. When $s < 0.7$, the errors are less than 10^{-15}—about the order of Cray's round-off error. Because s is the ratio of the dimensional Δv and the most probable speed, even a fairly coarse discretization produces little error.

Error Induced by Finite f_ε

If we suppose that $\Delta v \to 0$, i.e., the velocity space is continuous, then the relative errors in density and temperature induced by finite f_ε are

$$\left(\frac{\Delta \rho}{\rho}\right)_\varepsilon = \frac{4}{\pi^{1/2}} \int_x^\infty u^2 e^{-u^2} \, du$$

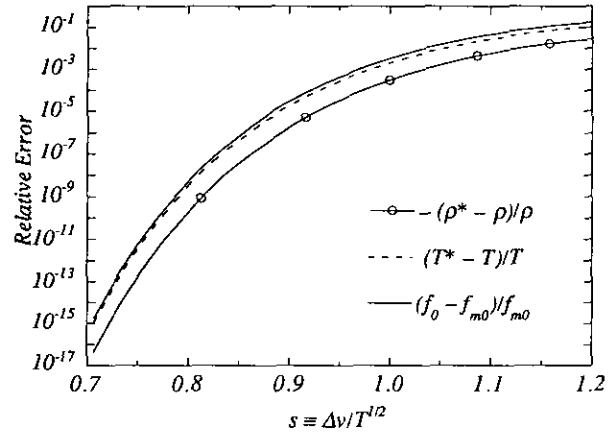

FIG. 3. Influence of Δv on errors in density, temperature, and value of the distribution function for the Maxwellian distribution.

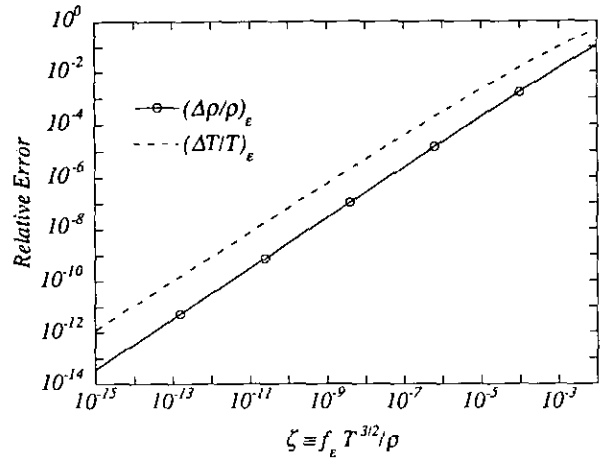

FIG. 4. Influence of f_ε on errors in density and temperature for the Maxwellian distribution.

and

$$\left(\frac{\Delta T}{T}\right)_\varepsilon = \frac{4}{\pi^{1/2}} \int_x^\infty u^4 e^{-u^2}\, du,$$

respectively, where $x \equiv \sqrt{-\ln[f_\varepsilon(\pi T)^{3/2}/\rho]} = \sqrt{-\ln[\pi^{3/2}\zeta]}$ with $\zeta \equiv f_\varepsilon T^{3/2}/\rho$. We plot the lines on Fig. 4. It can be seen that if ρ and T are $O(1)$, $f_\varepsilon < 10^{-5}$ is required to give an error of about 0.1% in density and temperature.

Estimation of N as a Function of s and ζ

When s and ζ are chosen for a specified accuracy, the number of important points N can be estimated using the fact that $N\,\Delta v^3$ is approximately the volume of the sphere whose radius R_0 is governed by $f_\varepsilon = \rho/(\pi T)^{3/2} \exp(-R_0/T)$ in velocity space. The result is

$$N = \frac{4\pi}{3} s^{-3} [-\ln \pi^{3/2}\zeta]^{3/2}$$

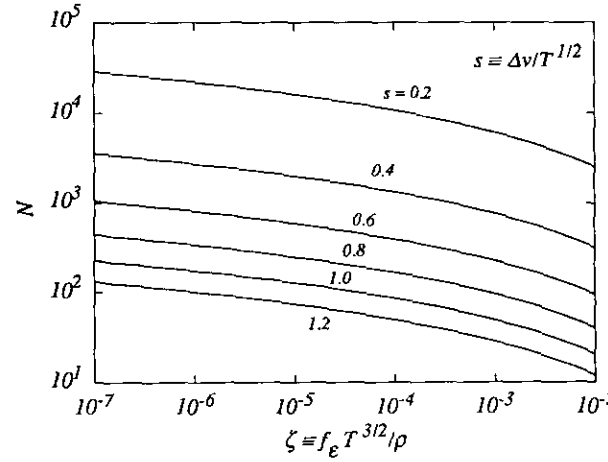

FIG. 5. Estimation of the number of nodes in the velocity space as a function of s and ζ.

and is shown in Fig. 5. The discussion above showed that one usually requires $s < 1$ and $\zeta < 10^{-5}$; hence we see that N should be between 10^2 and 10^4.

Choice of Parameters for General Distribution Functions

Unfortunately, the above error analysis is not applicable for arbitrary distribution functions. However, we may replace the density and temperature in the analysis above by estimated effective values. For example, if the distribution function does not deviate too strongly from a Maxwellian, then when the accuracy requirements $\Delta\rho/\rho$ and $\Delta T/T$ are given, Δv can be estimated using the minimum temperature in the flow field, while f_ε be estimated by the smallest $\rho/T^{3/2}$. Numerical experiments may be required if rough estimates of the density and temperature are not available.

7. EXAMPLES OF THE Δ-ε METHOD

Some applications of the method are presented below to demonstrate its accuracy and efficiency and to detect possible deficiencies.

Relaxation of a Homogeneous Gas to Equilibrium

As the first application of the Δ-ε method, we studied a homogeneous relaxation problem for which an analytical solution was found by Krook and Wu [18]. The distribution function for VHS molecules with $\kappa = 4$ is

$$f(v, t) = \frac{1}{2K(2\pi K)^{3/2}} \left(5K - 3 + \frac{1-K}{K} v^2\right) \exp(-v^2/2K), \qquad t \geq 0, \tag{18}$$

where $v = \|v\|$, and $K = 1 - 0.4 \exp(-t/6)$. Nanbu [4] calculated this problem using his simulation method.

In our calculation using the Δ-ε method, the number of integration points M was 40,000. The nondimensional cell size Δv in velocity space was 0.5, $f_\varepsilon = 10^{-6}$ and the nondimensional time step was $\Delta t = 0.05$. In Fig. 6 the velocity distribution function is plotted and compared with the analytical solution of Krook and Wu. Very good agreement is found at all times.

Note that unlike Nanbu [4], no averaging procedure was applied to exploit the spherical symmetry of the problem in our calculations. Good results are obtained on all positive and negative axes. We note that the Δ-ε solution is in good agreement with Krook and Wu's exact solution at large time ($t = 100$). In contrast, Nanbu found the poorest agreement between his distribution function and the exact solution at the largest time of his calculation ($t = 8.4$).

At $t = 100$ (after about 100 collisions), the Krook–Wu solution is essentially at equilibrium. Figure 6 indicates that

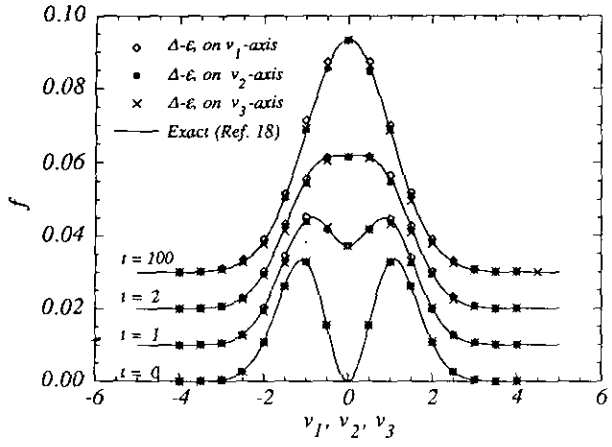

FIG. 6. Comparison of the distribution function calculated by the Δ-ε method with the exact solution of Krook and Wu [18]. Note that the data for $t \geqslant 1$ have been shifted upward in the figure for clarity.

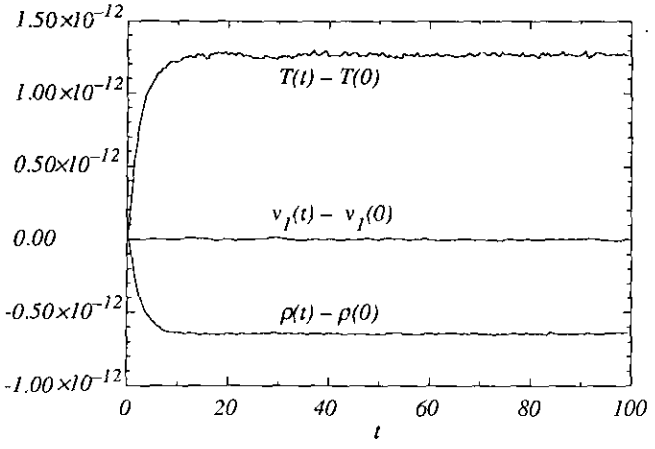

FIG. 8. History of the moments changes for the Krook–Wu problem; $\Delta v = 0.5$.

the equilibrium state of the discrete velocity gas in indistinguishable from a Maxwellian. This result agrees with the analysis above, and the study of Goldstein *et al.* [14]. When $\Delta v = 1$, the agreement between the equilibrium states is still good (Fig. 7). However, for larger Δv ($=\frac{4}{3}$), the equilibrium state of the discrete velocity gas appears to be far from the correct one. Since in this case $s = 2\sqrt{2}/3 \approx 0.94$, the equilibrium should be very close to Maxwellian according to our previous error analysis. The reason for the discrepancy is that this Δv is simply too large to give correct moments of the non-Maxwellian distribution at $t = 0$. In fact, the density was 0.9734 instead of 1 and the temperature was 2.1177 instead of 2. If we compare the Maxwellian distribution with the appropriate moments

$$f(v) = 0.9734(2 \times 2.1177)^{-3/2} \exp(-v^2/2.1177)$$

while the computation at $t = 100$, the agreement is excellent.

The variation of density, x-velocity, and temperature with t is plotted on Fig. 8. It can be seen that all of them are almost strictly conserved because both Δv and f_ε are so small that the error they induced is even smaller than the fluctuations in the figure. The small fluctuations are believed due to computer round-off errors. At small t the errors in density and temperature are smaller because the round-off errors in the last several digits have not been saturated (i.e., they have not become random yet). This problem required about 87 s of CPU time on a Cray Y-MP/864 computer, for 2000 time steps.

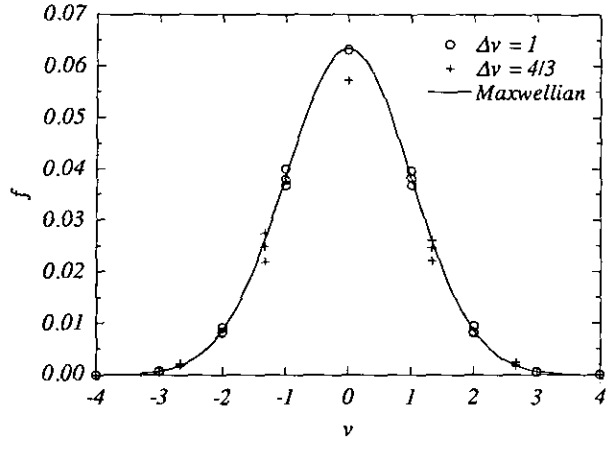

FIG. 7. Influence of Δv on equilibrium discrete distribution function.

Collision Integrals of a Bimodal Distribution Function

As a test for the accuracy of the Δ-ε method for calculating the collision integrals, we considered the following bimodal distribution function

$$f(v, t) = \frac{1}{\pi^{3/2}} \exp[-(v_1 - 1)^2 - v_2^2 - v_3^2] + \frac{1}{\pi^{3/2}} \exp[-(v_1 + 1)^2 - v_2^2 - v_3^2]. \quad (19)$$

In this example, the power κ of the intermolecular potential with the VHS model was taken to be 4 (Maxwell molecules), and $\mathrm{Kn} = C_\kappa$.

Figure 9 shows the distributions of A and B on the v_1-axis. For the Δ-ε calculation we used $\Delta v = 0.5$, $M = 10^5$, and the calculations were repeated 200 times using different sequences and then averaged. The distribution of the Boltzmann collision integral, is plotted in Fig. 10. It can be seen that there is very good agreement between the Δ-ε results and the exact solutions in both figures. In Fig. 10 we also plot the results using fewer integration points ($M = 10^3$) but use more (2×10^4) repetitions, keeping the total number of points unchanged. Little difference is observed. The influence of the number of integral points on the collision integral calculation is shown in Fig. 11. It

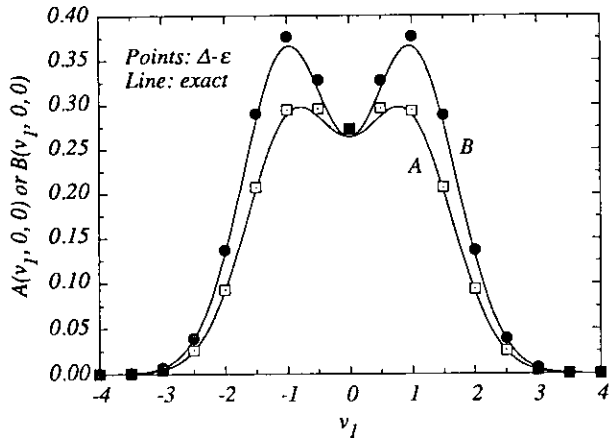

FIG. 9. Distributions of the replenishing (A) and depleting (B) parts of the collision integral on v_1-axis for a bimodal distribution function.

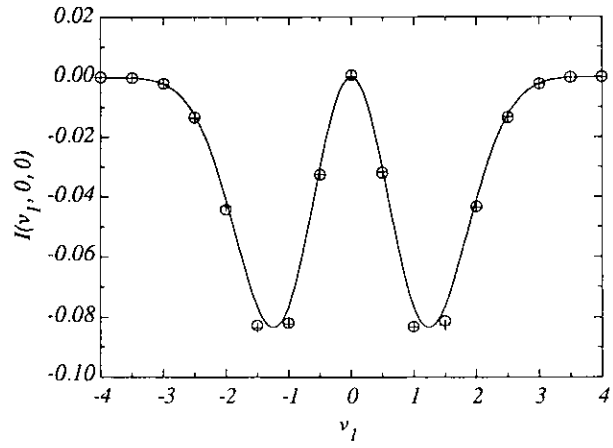

FIG. 10. Distribution of the collision integral on v_1-axis for a bimodal distribution function. Circles—$M = 10^5$ with 200 repetitions; crosses—$M = 10^3$ with 2×10^4 repetitions; line—exact.

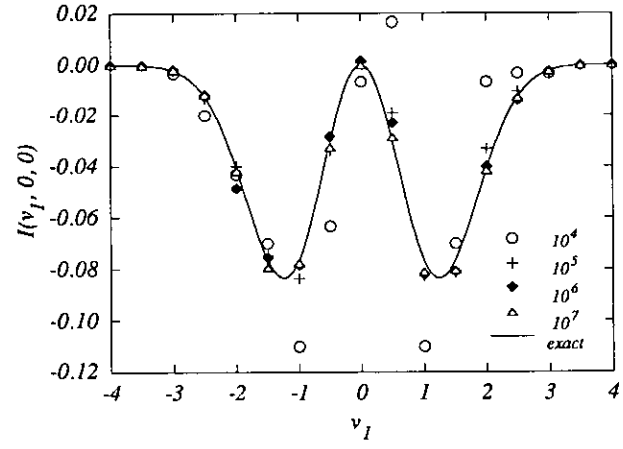

FIG. 11. Influence of the number of integral points on accuracy of collision integral calculations for a bimodal distribution function.

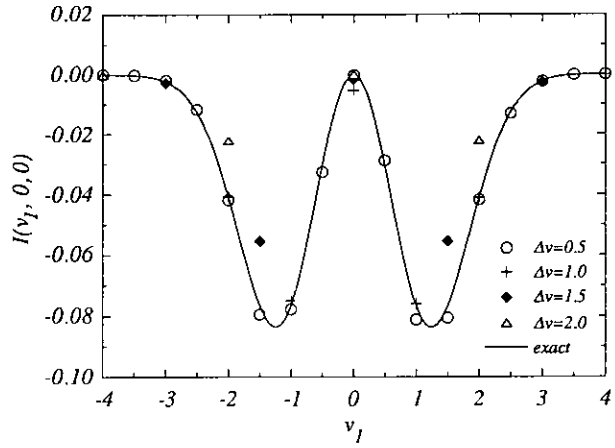

FIG. 12. Influence of Δv on accuracy of collision integral calculations for a bimodal distribution function.

can be seen that the integral is computed with acceptable accuracy for $M \geqslant 10^5$.

The influence of different Δv on the accuracy of the collision integral computation is shown in Fig. 12. Because of the bimodal shape of the distribution function, smaller Δv ($\leqslant 1$) is required to produce a specified accuracy in the collision integral than that estimated from the previous error analysis of the moments of the Maxwellian distribution. However, the results show that the Maxwellian estimate is a reasonable first guess. The influence of f_ε on the solution is shown in Fig. 13. As in the Maxwellian case, $10^{-4} < f_\varepsilon < 10^{-6}$ is a good choice.

The convergence and efficiency of the algorithm for the collision integral were also studied using this example. The zeroth and second moments $\langle B \rangle$ and $\langle Bv^2 \rangle$ computed by the sampling method were compared to the exact summation (Eq. (12)) and errors are plotted in Fig. 14. It can be seen that the convergence rate is between $M^{-1/2}$ and M^{-1}. A plot of CPU time versus M is depicted in Fig. 15. We see

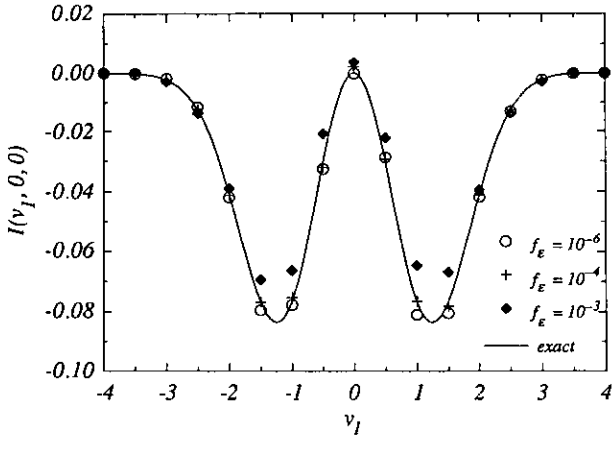

FIG. 13. Influence of f_ε on accuracy of collision integral calculations for a bimodal distribution function.

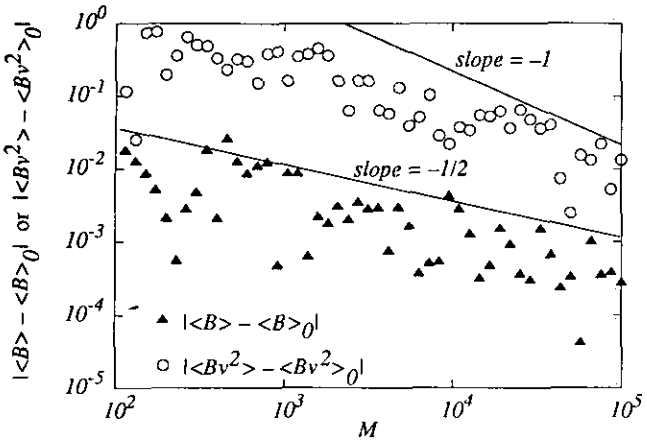

FIG. 14. Error of the moments due to Monte-Carlo approximation to the discrete collision integrals. $\langle\ \rangle$ were calculated by Monte-Carlo method, and $\langle\ \rangle_0$ were calculated using Eq. (12).

that the computer time is asymptotically proportional to M and the performance is about 0.66 million integral points per second, or 1.2 billion collisions per hour, on a Cray Y-MP/864 computer. (Note that M corresponds to the number of collisions in the direct simulation methods.) Further improvements in performance are possible because our code has not been fully optimized.

The Rayleigh Problem

The unsteady 1D Rayleigh problem has been solved by several authors using different models and methods [3, 19, 20]. The system consists of a semi-infinite gas above a flat plat at $y = 0$. The gas and plate are initially static, with $\rho = 1$ and $T = 1$. At time $t = 0^+$ the plate is impulsively moved and heated, and subsequently it is maintained at $v_1 = 2$ and $T = 1.6$. The reflection on the plate is assumed to be diffuse.

The solution of the Rayleigh problem based on Boltzmann collision processes for hard sphere molecules was first given by Bird [3]. We used the original program given by Bird [3] to obtain results with 40 cells at $t = 1$, 5, and 10. The total CPU time was 2640 s on a Cray Y-MP computer. The Δ-ε solution was obtained with $\Delta v = 0.75$, $M = 20{,}000$, $N_x = 21$, and $\Delta t = 0.1$. The total CPU time was about 90 s on the same Cray computer.

The results are compared in Figs. 16a, b. Very good agreement is found between the DSMC and Δ-ε solutions for the density, parallel velocity, and temperature profiles. The normal velocity profiles provide the most sensitive test of the computations and the agreement between the predictions of the two methods is fair.

Although a much shorter computer time was used, the Δ-ε results are smoother than the DSMC results in the far field region, indicating smaller statistical fluctuation. The comparison of the CPU times is not conclusive because the DSMC method has been improved [21–23], and the CPU time using a modern DSMC code should be much shorter. However, we believe that the performance of the Δ-ε code

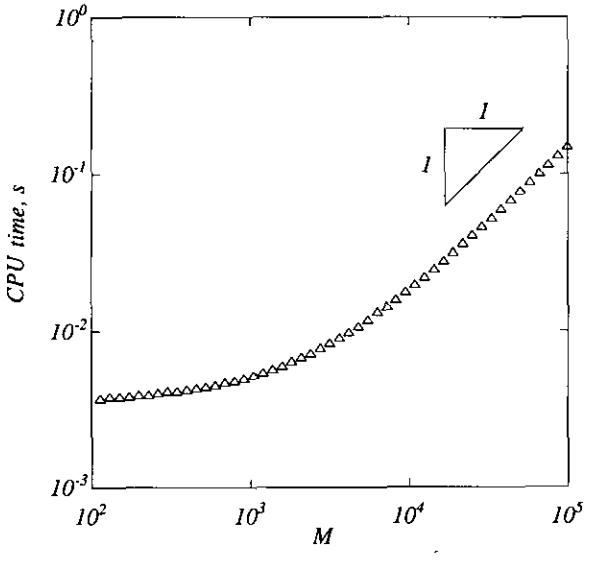

FIG. 15. Influence of the number of integration points on CPU time on a Cray Y-MP/864.

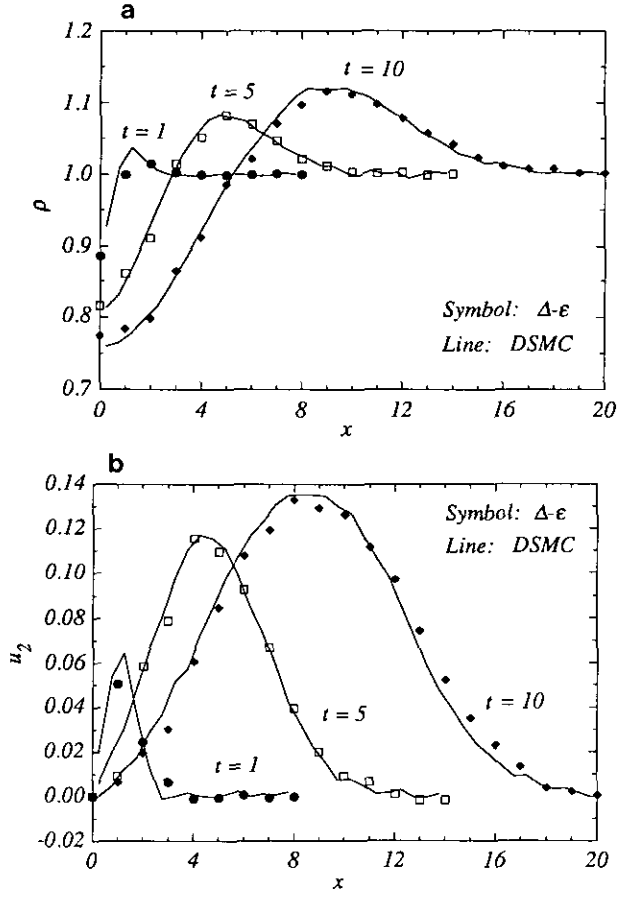

FIG. 16. The 1D Rayleigh problem. Comparison between the Δ-ε solution and the DSMC solutions: (a) density; (b) normal velocity.

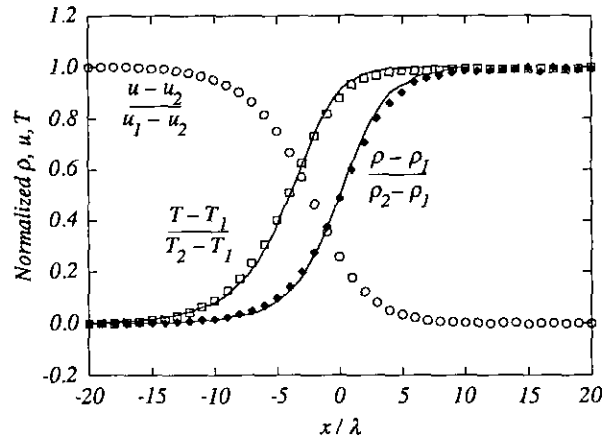

FIG. 17. Internal structure of a normal shock. VHS molecules with $\kappa = 4$; $M = 3$: Line, Baganoff and McDonald [23]; points, Δ-ε.

can also be greatly improved in the future, since little has been done to optimize the code.

Internal Structure of Normal Shock Waves

The problem of the structure of 1D normal shock waves has been widely used as a test for new algorithms for the Boltzmann equation. In this work the gas was initially at the upstream equilibrium state in the left half-space and in the downstream equilibrium state in the right half-space. The downstream state was determined from the upstream state using the Rankine–Hugoniot relations. The infinite physical space $-\infty < x < +\infty$ was truncated to a finite region $-l < x < l$ (nondimensionalized by the upstream mean free path). In our calculation, VHS molecules with $\kappa = 4$ were assumed. The Mach number was 3. This problem was also calculated by Baganoff and McDonald [23]. In the present Δ-ε calculation, we took $\Delta v = 0.7185$, $\Delta t = 0.025$, $l = 40$, and $\Delta x = 1$. The number of integration points used for each spatial node is 10,000.

We stopped the calculation after 1100 time steps, when the rms difference in density between the last two steps was about 3.74×10^{-5}. Figure 17 shows the density, velocity, and temperature profiles of our results as well as those of Baganoff and McDonald. The agreement is excellent. The Rayleigh line

$$P_{xx} = 1 + 2U^2_{\infty u,x}\left(1 - \frac{1}{\rho}\right)$$

has been used as a sensitive test of the absolute accuracy of shock structure by Goldstein *et al.* [14]. The Rayleigh line was accurately reproduced by our method (Fig. 18). The CPU time for this problem was 1777 s on a Cray Y-MP computer.

Two-Dimensional Flow Past an Adiabatic Cylinder

As the last application of the Δ-ε method, we consider two-dimensional supersonic flow past a circular cylinder. The DSMC solution to this problem was given by Crawford and Vogenitz [24].

In this problem, the Mach number of the incoming flow is 5.46 and the Knudsen number based the cylinder diameter is 0.3. The gas is modeled as VHS molecules with $\kappa = 11$. The cylinder surface is diffusely reflecting and has a dimensionless temperature of 11.23.

In the Δ-ε calculation, the computational domain was taken as $\{0.5 \leqslant r \leqslant 2; 0 \leqslant \theta \leqslant \pi\}$, where r is the radius nondimensionalized by the diameter $2R$ of the cylinder, and θ is the angle measured clockwise from the stagnation point. The domain was evenly divided into 14×19 cells, giving 3000 grid points. Other computational parameters used were: $\Delta v = 0.9147$, $M = 10{,}000$, and $\Delta t = 0.01$. The rms difference in density between the last two steps after 200 time steps was 1.70×10^{-4}. The total CPU time used was 5722 s on a Cray Y-MP computer.

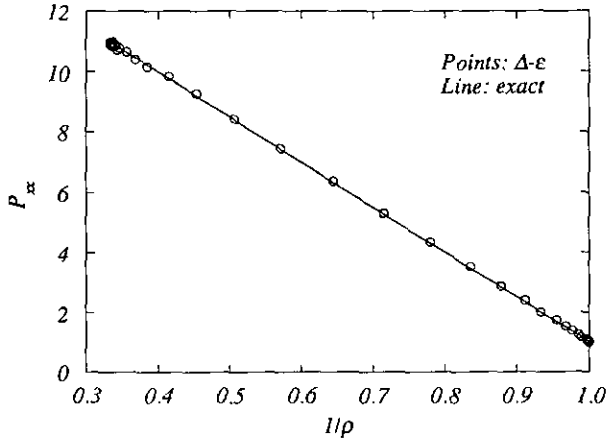

FIG. 18. The Rayleigh line by the Δ-ε method compared with the analytical solution for a normal shock at $M = 3$ in a VHS gas of Maxwell molecules ($\kappa = 4$).

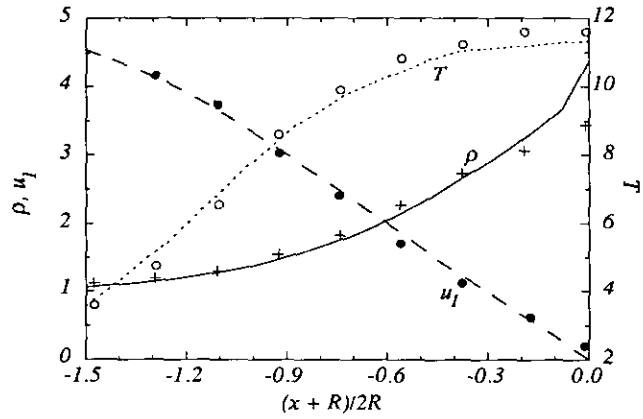

FIG. 19. Mach 5.46 flow past an adiabatic cylinder. Macroscopic quantities along the stagnation line by the Δ-ε method compared with the DSMC solution [24]: points, DSMC; line, Δ-ε.

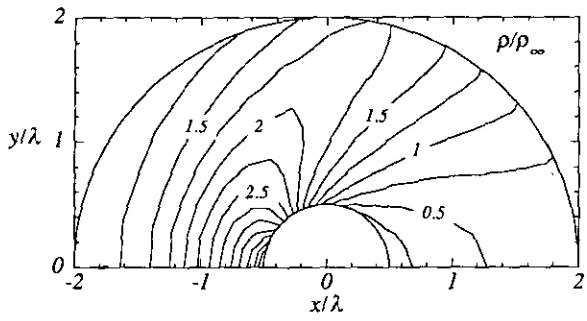

FIG. 20. Density contours computed by Δ-ε method for Mach 5.46 flow past an adiabatic cylinder.

The density, velocity, and temperature profiles along the stagnation line are shown in Fig. 19 along with the results of Crawford and Vogenitz. Although Crawford and Vogenitz used the inverse power law model rather than the VHS model, very good agreement is found for all quantities. The only significant difference between the calculations is in the density near the wall.

The density contours are plotted in Fig. 20. The solution is seen to be very smooth, partially because our method is more deterministic than direct simulation methods and partially because more elements in physical space were used than in the DSMC calculation. The bow shock can be identified but is quite thick. This indicates that most of the flow field is far from equilibrium.

7. CONCLUSIONS

In this paper we have described the Δ-ε frame and corresponding algorithms for the Boltzmann equation in this new frame. In the frame one considers only the important distribution function points while maintaining the advantages of discrete velocity methods. This makes it more efficient than traditional discrete velocity methods, especially for large Mach number flows. The method can be extended to more complex problems (e.g., multi-component gases and gas with internal energy). Many available numerical methods for hyperbolic equations can be directly applied for the convection terms. The method also allows easier coupling with Navier–Stokes or Euler equations to simulate flows with a large span of mean free paths.

The scheme used to approximate the collision integral has fair convergence rate and the computer time needed is proportional to the number of integral points. The choice of the number of integral points is quite flexible and this enables one to adjust the number at different locations according to accuracy requirements. Numerical calculations show that the Δ-ε method gives very smooth results. The statistical fluctuations of the method are less than those of the direct simulation methods. The method is very efficient for unsteady problems. However, it is less efficient than the direct simulation methods for steady state problems. Its efficiency for steady state problems could be greatly improved by employing unstructured grids and acceleration schemes such as multi-grid iterations.

The efficiency of the Δ-ε discretization could be further improved if nonuniform discretization in velocity space were used. The ultimate strategy would probably be to use adaptive discretizations so that large elements were automatically used in slowly changing regions and small elements used in rapidly changing regions. This, of course, would require a complex data structure and complex algorithms that remain to be developed.

APPENDIX A: GENERATION OF THE TABLE USED FOR POST-COLLISION VELOCITIES

For a pair of pre-collision velocities $\mathbf{i}\,\Delta v$ and $\mathbf{j}\,\Delta v$, the post-collision velocities $\mathbf{k}\,\Delta v$ lie on a sphere, i.e.,

$$(\mathbf{i}+\mathbf{j}-2\mathbf{k})^2=(\mathbf{i}-\mathbf{j})^2, \qquad \mathbf{i},\mathbf{j},\mathbf{k}\in\mathbb{Z}^3,$$

or

$$(\mathbf{k}-\mathbf{i})\cdot(\mathbf{k}-\mathbf{j})=0 \tag{A1}$$

which is equivalent to the two forms,

$$(\mathbf{k}-\lfloor\mathbf{i},\mathbf{j}\rfloor)^2-(\mathbf{k}-\lfloor\mathbf{i},\mathbf{j}\rfloor)\,|\mathbf{i}-\mathbf{j}|=0 \tag{A2}$$

and

$$(\mathbf{k}+\lceil\mathbf{i},\mathbf{j}\rceil)^2-(\mathbf{k}+\lceil\mathbf{i},\mathbf{j}\rceil)\,|\mathbf{i}-\mathbf{j}|=0, \tag{A3}$$

where we have defined

$$\begin{aligned}\lfloor\mathbf{i},\mathbf{j}\rfloor&=(\mathbf{k}\in\mathbb{Z}^3\,|\,k_s=\min(i_s,j_s),\ s=1,2,3),\\ \lceil\mathbf{i},\mathbf{j}\rceil&=(\mathbf{k}\in\mathbb{Z}^3\,|\,k_s=\max(i_s,j_s),\ s=1,2,3),\end{aligned} \tag{A4}$$

and

$$|\mathbf{i}|=(\mathbf{k}\in\mathbb{Z}^3\,|\,k_s=|i_s|,\ s=1,2,3).$$

Therefore, if for each $\mathbf{j}\geqslant 0$ we can find the set

$$\mathrm{I}_\mathbf{j}=\{\mathbf{i}\in\mathbb{Z}^3\,|\,\mathbf{i}^2=\mathbf{i}\cdot\mathbf{j}\}; \tag{A5}$$

then the set of post-collision velocity pairs $(\mathbf{i}',\mathbf{j}')$ is

$$\begin{aligned}\mathrm{K}_{\mathbf{ij}}=\{(\mathbf{i}',\mathbf{j}')\in\mathbb{Z}^3\times\mathbb{Z}^3\,|\,&\mathbf{i}'=\lfloor\mathbf{i},\mathbf{j}\rfloor+\mathbf{s},\\ &\mathbf{j}'=\lceil\mathbf{i},\mathbf{j}\rceil-\mathbf{s},\ \mathbf{s}\in\mathrm{I}_{|\mathbf{i}-\mathbf{j}|}\}.\end{aligned} \tag{A6}$$

The reason that we use (A2) and (A3) instead of (A1) is that the table of $\mathrm{I}_\mathbf{j}$ need only be calculated for nonnegative $\mathbf{j}$. This

reduces the table length by about a factor of 8. The recovery of the post-collision velocities from the table is very easy. Further reduction in table length is possible by exploiting additional symmetry properties. However, the recovery becomes more difficult and the additional computer time needed for the recovery in calculating the collision integrals makes such reduction undesirable.

The table $\mathrm{I}_{\mathbf{j}}$ for a set of $\mathbf{j}$ must be calculated. We take $\mathbf{j}$ to be the integer nodes in the box $[0, N_d]^3$, where N_d is chosen so that $N_d \Delta v$ is large enough that all important points lie in the box. Rewrite $\mathbf{i}^2 = \mathbf{i}\cdot\mathbf{j}$ as $(2\mathbf{i}-\mathbf{j})^2 = \mathbf{j}^2$. A brute force calculation of this problem would require $O(N_d^6)$ effort. If we view $2\mathbf{i}-\mathbf{j}$ as unknown and $\mathbf{j}^2$ as known; however, we can solve the problem in two steps. In the first step, we solve the sum of three integers problem numerically (cf. [25]),

$$\mathbf{k}^2 = \mathbf{j}^2 \qquad \text{for} \quad k_1 \geqslant k_2 \geqslant k_3 \geqslant 0, \tag{A7}$$

for $\mathbf{j}^2$ from zero to $3N_d^2$. This step is very fast for small to moderate N_d, in spite of the $O(N_d^5)$ effort needed. In the second step the members of $\mathrm{I}_{\mathbf{j}}$ are calculated by

$$\mathbf{i} = \frac{\mathbf{i}+\mathbf{k}^*}{2} \qquad \text{if} \quad j_s \equiv k_s^* \pmod 2, \quad s = 1, 2, 3, \tag{A8}$$

where $\mathbf{k}^*$ is obtained by permuting the indices of $\mathbf{k}$. This second step requires an N_d^3 effort and therefore it is very fast.

In practice the table $\mathrm{I}_{\mathbf{j}}$ for all $\mathbf{j}$ is collected as a 3D array instead of a 6D array. In Fig. A1 the total table length and corresponding CPU time for typical N_d are shown. It can be seen that the table length varies slightly faster than the number of nodes. The CPU time is quite short so pre-saving the data on the disk is unnecessary. If brute force were used, the CPU time for $N_d = 20$ would be more than 300 s instead of about 1 s.

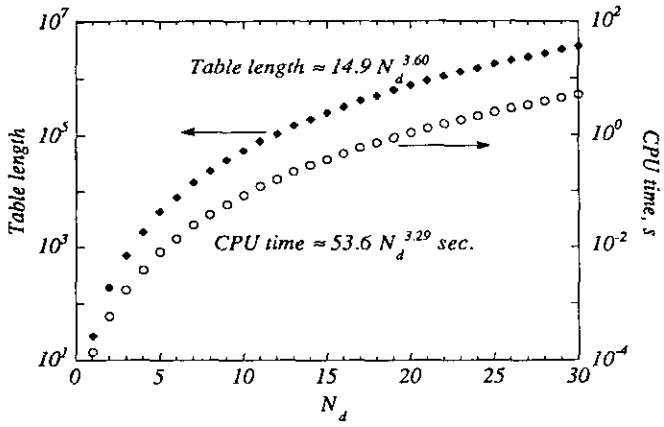

FIG. A1. CPU time on a Cray Y-MP/864 needed for generating the tables of post-collisional discrete velocities and the corresponding table lengths.

APPENDIX B: CALCULATION OF THE COLLISION INTEGRAL A AND B FOR A BIMODAL DISTRIBUTION FUNCTION WITH $\kappa = 4$

For the distribution function given by Eq. (20), $f(\mathbf{v}) = 2\pi^{-3/2}\exp(-v^2-1)\cosh 2v_1$, the replenishing part of collision integral, A, is

$$\begin{aligned} A(\mathbf{v}) &= \frac{4}{\pi^3}\int_{S^2}\int_{\mathbb{R}^3} e^{-\mathbf{v}'^2-\mathbf{w}'^2-2}\cosh 2v_1'\cosh 2w_1'\,d\mathbf{w}\,\frac{d\Omega}{4\pi} \\ &= \frac{2}{\pi^3}\int_{S^2}\int_{\mathbb{R}^3} e^{-\mathbf{v}'^2-\mathbf{w}'^2-2}[\cosh 2(v_1'+w_1') \\ &\quad + \cosh 2(v_1'-w_1')]\,d\mathbf{w}\,\frac{d\Omega}{4\pi}. \end{aligned}$$

Note that

$$\begin{aligned} &\frac{2}{\pi^3}\int_{\mathbb{R}^3} e^{-\mathbf{v}^2-\mathbf{w}^2-2}\cosh 2(v_1'+w_1')\,d\mathbf{w} \\ &\quad = \frac{2}{\pi^3}\int_{\mathbb{R}^3} e^{-\mathbf{v}^2-\mathbf{w}^2-2}\cosh 2(v_1+w_1)\,d\mathbf{w} \\ &\quad = \frac{2}{\pi^{3/2}} e^{-\mathbf{v}^2-1}\cosh 2v_1, \end{aligned}$$

and

$$\begin{aligned} &\frac{2}{\pi^3}\int_{\mathbb{R}^3} e^{-\mathbf{v}^2-\mathbf{w}^2-2}\cosh 2(v_1'-w_1')\,d\mathbf{w} \\ &\quad = \frac{2}{\pi^3}\int_{\mathbb{R}^3} e^{-\mathbf{v}^2-\mathbf{w}^2-2}[\cosh 2(v_1-2n_1\mathbf{n}\cdot\mathbf{v}) \\ &\quad \times \cosh 2(w_1-2n_1\mathbf{n}\cdot\mathbf{w}) + \sinh 2(v_1-2n_1\mathbf{n}\cdot\mathbf{v}) \\ &\quad \times \sinh 2(w_1-2n_1\mathbf{n}\cdot\mathbf{w})]\,d\mathbf{w} \\ &\quad = \frac{2}{\pi^3}\int_{\mathbb{R}^3} e^{-\mathbf{v}^2-\mathbf{s}^2-2}[\cosh 2(v_1-2n_1\mathbf{n}\cdot\mathbf{v})\cosh 2s_1 \\ &\qquad + \sinh 2(v_1-2n_1\mathbf{n}\cdot\mathbf{v})\sinh 2s_1]\,d\mathbf{s} \\ &\qquad (\mathbf{s} \equiv \mathbf{w} - 2\mathbf{n}\mathbf{n}\cdot\mathbf{w}) \\ &\quad = \frac{2}{\pi^{3/2}} e^{-\mathbf{v}^2-1}\cosh 2(v_1-2n_1\mathbf{n}\cdot\mathbf{v}), \end{aligned}$$

where we have used the fact that $\mathbf{v}' = \mathbf{v} - \mathbf{n}\mathbf{n}\cdot(\mathbf{v}-\mathbf{w})$ and $\mathbf{w}' = \mathbf{w} - \mathbf{n}\mathbf{n}\cdot(\mathbf{w}-\mathbf{v})$. Finally we have

$$\begin{aligned} A(v) &= \frac{1}{\pi^{3/2}} e^{-\mathbf{v}^2-1} \\ &\quad \times \left(\cosh 2v_1 + \int_{S^2}\cosh 2(v_1-2n_1\mathbf{n}\cdot\mathbf{v})\,\frac{d\Omega}{4\pi}\right). \end{aligned}$$

The angular integral can be easily calculated with high precision using Gauss quadrature. The depleting part of the collision integral, B, is easy to evaluate and is

$$B(v) = \frac{4}{\pi^{3/2}} e^{-v^2-1} \cosh 2v_1.$$

ACKNOWLEDGMENTS

This work was supported by the Texas Advanced Research Program. Computing resources were provided by the University of Texas System Center for High Performance Computing.

REFERENCES

1. K. Aoki, in *Rarefied Gas Dynamics: Theoretical and Computational Techniques*, edited by E. P. Muntz *et al.* (AIAA, Washington, DC, 1989), p. 297.
2. T. J. Chung, *Finite Element Analysis in Fluid Dynamics* (McGraw-Hill, New York, 1978).
3. G. A. Bird, *Molecular Gas Dynamics* (Oxford Univ. Press, London, 1976).
4. K. Nanbu, *J. Phys. Soc. Jpn.* **49**, 2042 (1980).
5. H. Babovsky, *Math. Methods Appl. Sci.* **8**, 223 (1986).
6. A. Nordsieck and B. L. Hicks, "Monte Carlo Evaluation of the Boltzmann Collision Integral," in *Rarefied Gas Dynamics*, edited by C. L. Brundin (Academic Press, New York, 1967), p. 695.
7. S. M. Yen, *Annu. Rev. Fluid Mech.* **16**, 67 (1984).
8. V. V. Aristov and F. G. Tcheremissine, "The Kinetic Numerical Method for Rarefied and Continuum Gas Flows," in *Rarefied Gas Dynamics, Vol. 1*, edited by Belotserkovskii, *et al.* (Plenum, New York, 1985), p. 269.
9. Z. Tan, Y.-K. Chen, P. L. Varghese, and J. R. Howell, "New Numerical Strategy to Evaluate the Collision Integral of the Boltzmann Equation," in *Rarefied Gas Dynamics: Theoretical and Computational Techniques*, edited by E. P. Muntz *et al.* (AIAA, Washington, DC, 1989), p. 359.
10. T. Inamuro and B. Sturtevant, *Phys. Fluids A* **2**, 2196 (1990).
11. S. Chapman and T. G. Cowling, *The Mathematical Theory of Non-Uniform Gases*, 3rd ed. (Cambridge Univ. Press, Cambridge, 1970).
12. G. A. Bird, "Monte-Carlo Simulation in an Engineering Context," in *Rarefied Gas Dynamics, Part 1*, edited by S. S. Fisher (AIAA, New York, 1981), p. 239.
13. C. Cercignani, *Theory and Application of the Boltzmann Equation* (Elsevier, New York, 1975).
14. D. Goldstein, B. Sturtevant, and J. E. Broadwell, "Investigations of the Motion of Discrete-Velocity Gases," in *Rarefied Gas Dynamics: Theoretical and Computational Techniques*, edited by E. P. Muntz *et al.* (AIAA, Washington, DC, 1989), p. 100.
15. D. E. Knuth, *The Art of Computer Programming, Vol. 3* (Addison-Wesley, Reading, MA, 1973).
16. P. Bratley, B. L. Fox, and L. E. Schrage, *A Guide to Simulation*, 2nd ed. (Springer-Verlag, New York, 1987).
17. V. V. Aristov and F. G. Cheremisin, *USSR Comput. Meths. Math. Phys.* **20**, 208 (1980).
18. M. Krook and T. T. Wu, *Phys. Fluids* **20**, 1589 (1977).
19. C. K. Chu, "The High Mach Number Rayleigh Problem According to the Krook Model," in *5th Int. Symp. on Rarefied Gas Dynamics*, edited by C. L. Brundin (Academic Press, New York, 1967).
20. I. D. Boyd and J. P. W. Stark, *J. Comput. Phys.* **80**, 374 (1989).
21. G. A. Bird, "Perception of Numerical Methods in Rarefied Gas-dynamics," in *Rarefied Gas Dynamics: Theoretical and Computational Techniques*, edited by E. P. Muntz *et al.* (AIAA, Washington, DC, 1989), p. 211.
22. I. D. Boyd, P. F. Penko, and L. M. Carney, AIAA Paper-90-1693, *AIAA/ASME 5th Joint Thermophysics and Heat Transfer Conference, Seattle, WA, 1990* (unpublished).
23. D. Baganoff and J. D. McDonald, *Phys. Fluids A* **2**, 1248 (1990).
24. D. R. Crawford and F. W. Vogenitz, "Monte Carlo Calculations of the Shock Layer Structure on Adiabatic Cylinders in Rarefied Supersonic Flow," in *Rarefied Gas Dynamics* (DFVLR Press, Porz-Wahn, Germany, 1974).
25. D. E. Flath, *Introduction to Number Theory* (Wiley, New York, 1989).